Fluorescence Molecular Imaging

Heung-Kook Choi[a,b], Vasilis Ntziachristos[b], Ralph Weissleder[b]

[a]*School of Computer Engineering, Inje University, Gim-Hae, Korea*
[b]*Center for Molecular Imaging Research, Massachusetts General Hospital, Harvard Medical School, Charlestown, Massachusetts 02129, USA*

Abstract

The chemotherapy sensitive Lewis lung carcinoma (LLC) and chemotherapy resistant Lewis lung carcinoma (CR-LLC) tumors concurrently implanted in mice, and compare these findings with histological macroscopic observations against 3D reconstruction of Fluorescence Molecular Tomography (FMT) preformed *in vivo* on the same animals. For the 3D image reconstruction we used 32 laser source images, a flat image and 3D surface rendering that confused for 3D Fluorescence Molecular Imaging (FMI). A minimum of ten tissue sections were analyzed per tumor for quantification of the TUNEL-positive cells, cell-associated Cy5.5-Annexin and vessel-associated Alexa Fluor-Lectin. These are useful apoptosis and angiogenesis markers, and they serve as validation experiments to data obtained *in vivo*using a Cy5.5-Annexin V conjugate injected intravenously in chemotherapy-treated animals carrying the tumors studied histologically. We detected higher levels of apoptosis and corresponding higher levels of Cy5.5 fluorescence in the LLC vs. the CR-LLC tumors according to tissue depth and these findings confirm that *in vivo* staining with the Cy5.5-Annexing conjugate correlates well with *in vitro* TUNEL staining and is consistent with the higher apoptotic index expected from the LLC line. There appeared to be 1.38% more apoptosis for LLC than CR-LLC. Consequently there is good correlation between the histology results and *in vivo* fluorescence-mediated optical imaging. In conclusion the apoptotic images of 3D FMI were validated by microscopic histological image analysis. This is a significant result for the continuous progress of fluorescence 3D imaging research.

Keywords: Fluorescence molecular tomography, 3D image reconstruction, Lewis lung carcinoma, Apoptosis, TUNEL, Angiogenesis, Microscopic histological image analyses.

Introduction

Non-invasive fluorescence imaging has emerged in recent years as an important method for *in vivo* imaging in small animal research due to the development of bio-compatible fluorochromes with molecular specificity and of appropriate imaging systems and methods [1,2]. Light has been traditionally used for high-resolution imaging of histological slices using fluorescence microscopy and for tissue sectioning with confocal and multi-photon microscopy. In these investigations light in the visible spectral region is traditionally used. For probing deeper in tissue, fluorochromes that emit in the near infrared(NIR) are employed. This is because tissue penetration of several centimeters can be achieved in this spectral region due to low tissue absorption. Imaging in the NIR has led to a new family of optical imaging techniques that are low resolution but lead to significantly higher penetration depths and retain high molecular specificity [3,4]. Optical imaging of small animals is carried out with several elegant technologies including bioluminescence imaging [5,6], fluorescence protein imaging [7,8], enzyme upregulation imaging [9,10] and

receptor specific imaging [11]. Detection is performed either with planar imaging (photographic) systems or more advanced technologies using tomographic principles. The latter have been developed to overcome several limitations of planar imaging; i.e. lack of accurate quantification and inability to resolve depth.

FMIis a particular example of a fluorescence tomographic method that was developed recently for small animal imaging. The technology has shown the ability to image protease expression deep in tissues in animal models *in vivo* [12]. An important aspect of these developments is the establishment of appropriate methods to serve as gold standard for validating the macroscopic appearance of fluorescent probes with the underlying biology. Of particular importance in these investigations is that the same fluorescent agent used for *in vivo*staining can also be imaged microscopically after excising the tissues of interest. This can offer a direct evaluation of imaging results and is an important step towards the acceptance of these technologies in biomedical practice.

In this work we focused on evaluating macroscopic FMT findings of apoptosis with the underlying TUNEL stain microscopic appearance. Apoptosis, or programmed cell death, is a critical process for organ development, tissue homeostasis, and removal of defective cells *in vivo* and plays an important role in many diseases, including cancer [13]and it is of great importance in the study and development of treatment strategies. To carry out this correlation we employed an *in vivo* marker of apoptosis using a previously developed Annexin V [14,15] based reporter conjugated to the NIR fluorochrome Cy5.5 with emission peak at 690nm. We analysed in parallel the histological appearance of this marker with its *in vivo* appearance on 3D reconstructed FMT images and correlated these findings with *in vitro* TUNEL staining of the excised tumours using the Cy3 fluorochrome.

Methods and Materials

Cell culture and animal models

LLC cells and CR-LLC cells were propagated in 10% FBS(Fetal Bovine Serum) and DMEM(Dulbecco's Modification of Eagle's Medium).

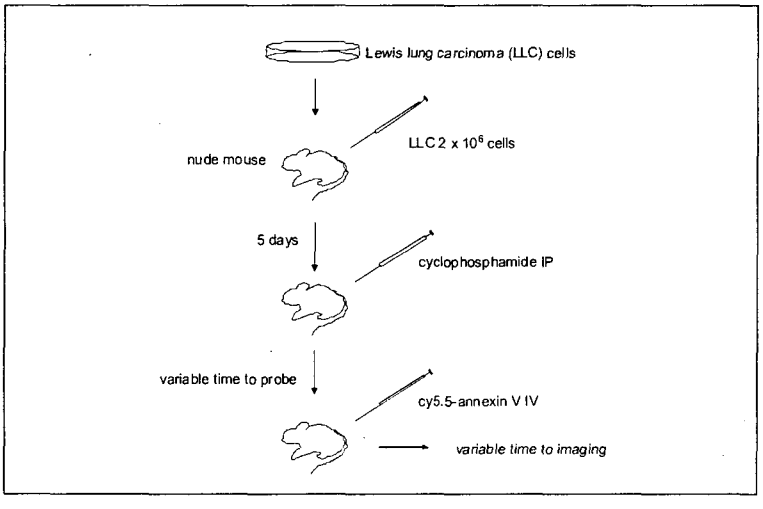

Figure 1. The biohistochemical stained animal model.

LLC and CR-LLC cells were implanted in female nu-nu mice. One million (10^6)cells were injected subcutaneously and bilaterally in the upper anterior thorax of the nude mice. Animals

were imaged 9-12 days after implantation, when tumors were 4-5 mm in diameter. Cyclophosphamide (Mead Johnson, Princeton, NJ) was administered as an i.p. injection at 170mg/kg. The first treatment was given 72 hours prior to imaging and the second treatment was given 24 hours prior to imaging. Cy5.5 labeled AnnexinV (at 1nmol/animal) was injected i.v. via tail vein injection two hours prior imaging (see Figure 1).

3D FMT image acquisition

FMT was performed using a parallel plate scanner previously developed [16]. The central piece of the system is the imaging chamber designed for small animals (see Figure 2). The system employs a constant intensity laser diode emitting at 672nm. The light source is time-shared amongst 32 fibers located at the back plate of the animal chamber and arranged into a 2cm1.5cm hexagonal grid. The back plate is moveable so that the object can be compressed against the front glass window if required. NIR detection is based on a NIR sensitive CCD camera (VersArray 512B, Roper Scientific Inc., Trenton, NJ) with 35mm f1.2 lenses (Nikon Inc., Melville, NY) and band-pass filters for emission and excitation measurements (705 nm and 671nm central wavelengths respectively, Andover Inc., Salem, NH). The CCD chip groups 512512 individual pixels, from which a central field of view is selected and appropriately binned each time to serve as a virtual detector grid.

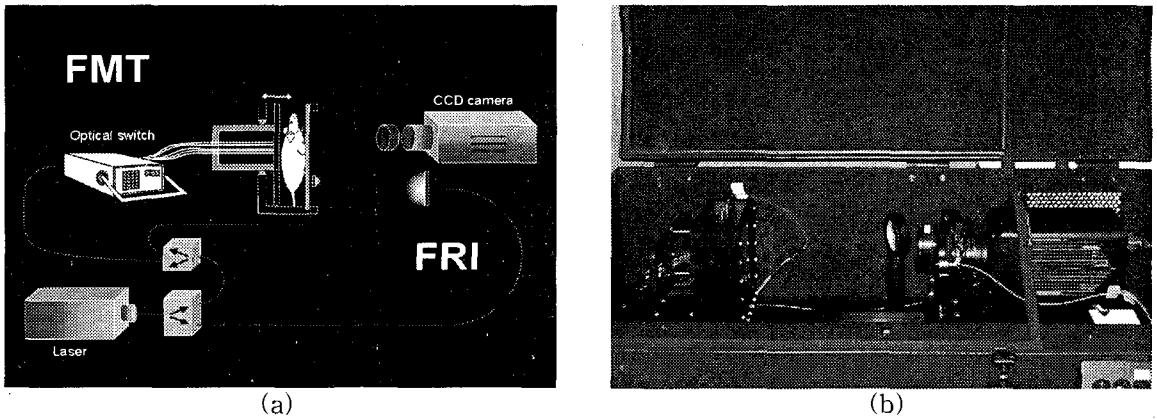

(a) (b)

Figure 2. (a) FMT and FRI architecture and (b) the system construction.

Imaging procedures involved placing the object or animal into the chamber and obtaining a front-illumination "photographic" image at the excitation wavelength with the NIR camera. This image was used to verify the subject's position and to detect four fiducial markers located on the back plate for automatic geometry extraction and image registration. The fiducial coordinates were also used to calculate the position of the fiber sources in relation to the object or animal. Then, the animal was surrounded by anoptical "matching fluid" consisting of intralipid and ink at appropriate concentrations to mimic the optical properties of the animal. Tomographic data were then obtained by capturing 64 transillumination images, acquired for 32 sources at the excitation and emission wavelengths respectively. Typical exposure times per source employed were 0.5 sec. at the excitation wavelength and 5 sec. at the emission wavelength corresponding to total imaging time of less than 5 minutes. The 3D image reconstruction was based on a normalized Born solution of the diffusion approximation previously described [12,17]. Inversion was based on the algebraic reconstruction technique that was run for 10 iterations on typical volumes consisting of a total of 104 source detector measurements and equal number of voxels. The three-dimensional datasets of the measurements were combined to create an image, which is shown in Figure 3.

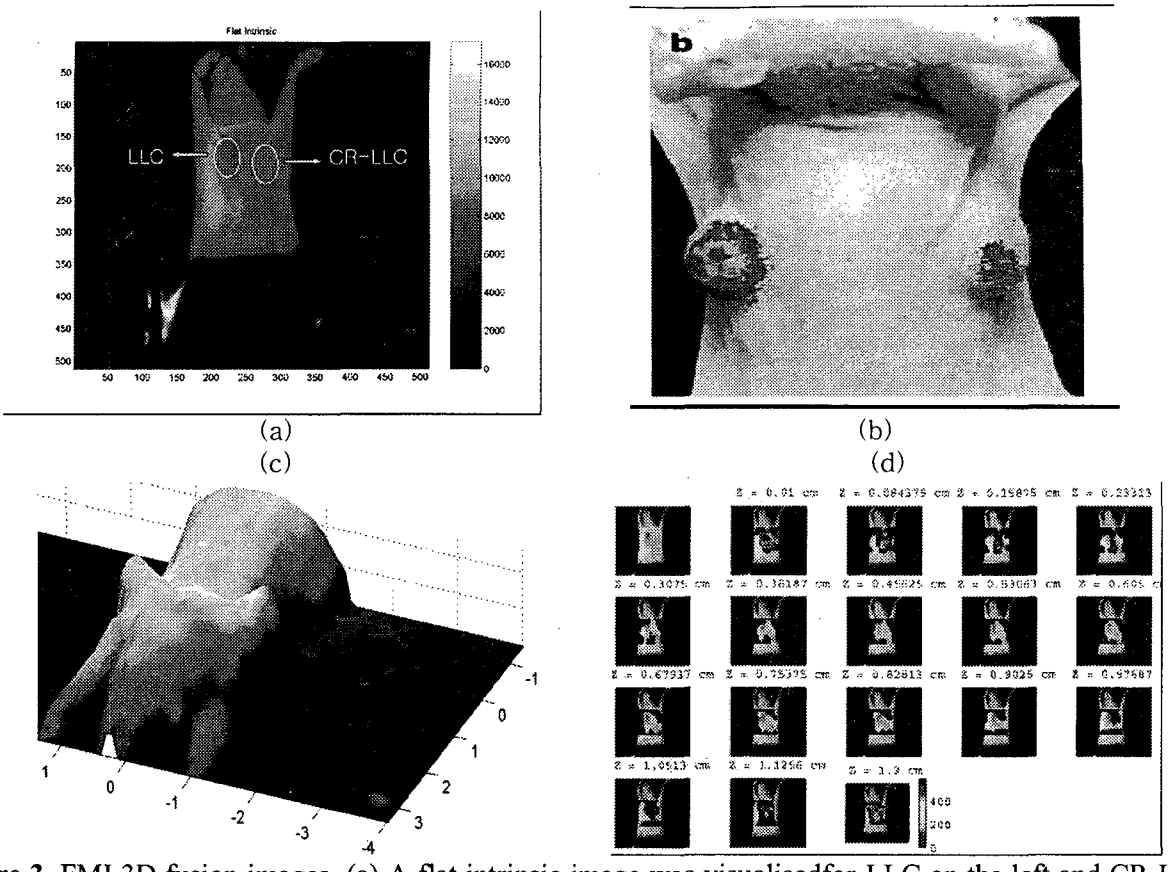

Figure 3. FMI 3D fusion images. (a) A flat intrinsic image was visualisedfor LLC on the left and CR-LLC on the right of the image, for M2. (b) The FMT fusion image. (c) 3D surface rendering. (d) The characterised FMT *in vivo* images according to the tissue depth.

Histological staining

The mice were preinjected with Alexa Fluor 488 -labeled lectin (Lycopersicon Esculentum, Vector Laboratories) at 100 g/animal ~15 min before sacrificing to reveal tumor blood vessels. Tumors excised from euthanized animals were snap frozen, and cut into 10-m sections. We stained the tumor sections for apoptosis using the terminal deoxynucleotidyl transferase-mediated nick end labeling(TUNEL) assay [18,19], which is provided in the ApopTag Apoptosis Detection Kit Manual (Serologicals Corporation, Norcross, GA). We followed the procedure for indirect staining of unfixed tissue cryosections. The apoptotic cells were stained with Cy3 and imaged using a fluorescence microscope. At leastminimum of ten tissue sections were analyzed per tumor for quantification of TUNEL-positive cells, cell-associated Cy-Annexin and vessel-associated Alexa Fluor-Lectin. TUNEL analysis performed on histology sections of the cyclophosphamide resistant tumors showed a lower incidence of apoptotic cells and a lower density of tumor blood vessels (lectin staining) than the sections of the tumors sensitive to chemotherapy. The *in situ*staining of DNA strand breaks detected by the TUNEL assay and subsequent visualization by light microscopy gives biologically significant data about apoptotic cells, which may be a small percentage of the total population [20]. Apoptotic cells stained positive with ApopTag Kits are easier to detect and their identification in more certain, as compared to the examination of simply histochemically stained tissues.

Microscopic image acquisition

Fluorescence microscopy with 10 magnification been performed using an inverted microscope (Zeiss Axiovert 100 TV, Wetzlar, Germany) fitted with appropriate filter sets (Omega Optical) i.e. 505 nm (490 nm~520 nm) for AF488, 560 nm (552 nm ~ 565 nm) for Cy3 and 680 nm (650 nm ~ 667 nm) for Cy5.5. Images were acquired using a Photometrics CH250 CCD (Photometrics, Tucson, AZ), with image acquisition and storage controlled by IP LabSpectrum software (Signal Analytics). The camera resolution was 10351316 pixels at 12 bits per pixel. The total analyzed histological images were 96. They were 51 images for the LLC and 45 images for the CR-LLC of the three nude mice and staining Cy5.5 and Cy3 respectively. Table I shows the total experimental and categorized images.

Table I The three nude mice of M1, M2 and M3 and each mouse of two different tumors that stained by Cy5.5 and Cy3.

Mouse No.	M1		M2		M3		Total
Stain\Carcinoma	LLC	CR-LLC	LLC	CR-LLC	LLC	CR-LLC	
Cy5.5	5	5	6	6	11	10	43
Cy3	. 10	10	5	5	14	9	53
Total	15	15	11	11	25	19	96

Image Analysis

Image processing and analysis was performed using the Visual C++ based IMAN (IMage ANalyzer, MedIT, Korea) run on a 2.2 GHz Pentium IV personal computer. For all histological slices a central 512512 region of interest was selected to avoid inhomogeneous boundaries and ensure homogeneous illumination. Images were converted to 8 bits description per pixel for handling speed and simplicity. Figure 4 shows the representative stained categorizing.

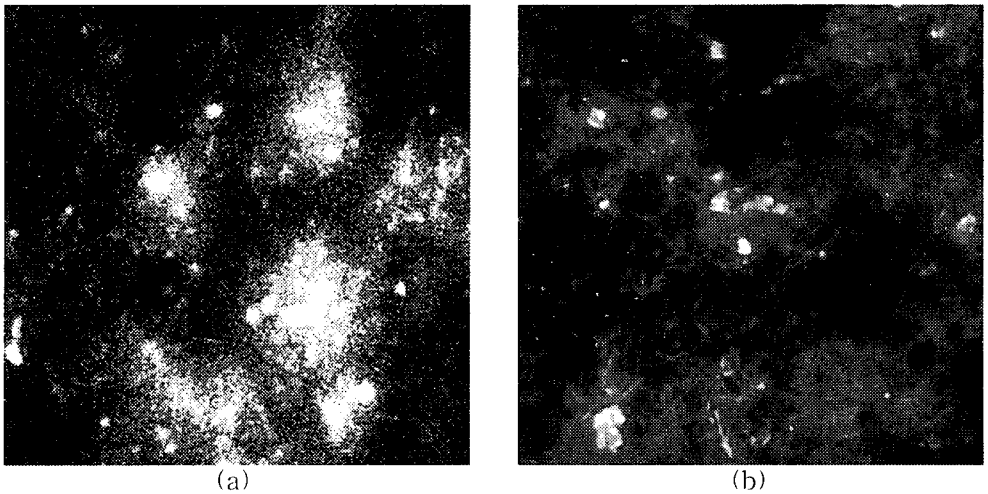

(a) (b)

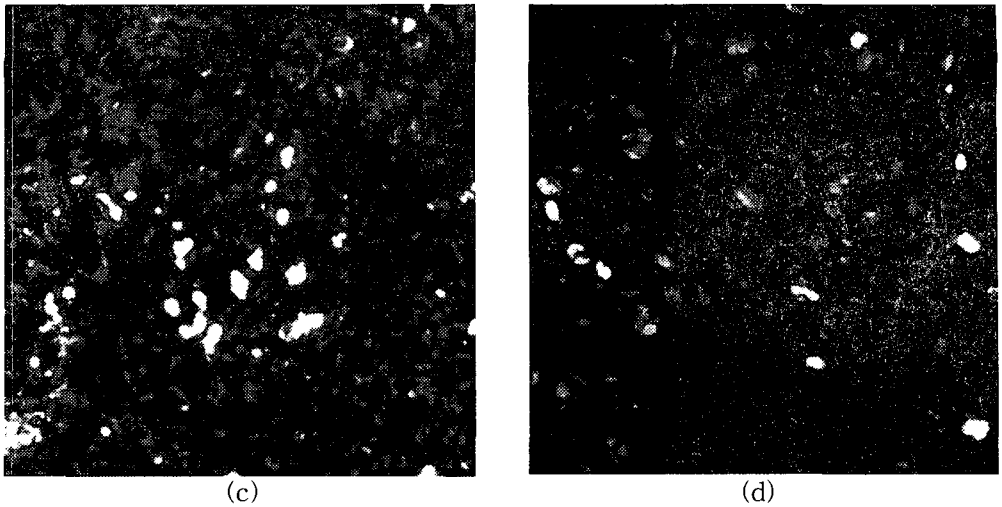

(c) (d)

Figure 4. Representative fluorescence microscopic images, 512 x 512 pixels, 8 bits per pixel. (a) LLC/Cy3. (b) CR-LLC/Cy3. (b) LLC/Cy5.5. (d) CR-LLC/Cy5.5.

Segmentation Histogram equalisation was applied to all images before applying the same threshold to convert images to binary [21].This process ensures that absolute image maxima, which vary significantly from study to study owing to varying illumination strength and staining conditions, do not affect the calculation. LLC images could not be segmented for any objects because of the high threshold value. CR-LLC images were notsegmented because of the low threshold value. Accordingly, LLC images display too few objects, and CR-LLC images display too many objects. Consequently the threshold was determined based on a training set of TUNEL-stained images obtained from studies performed prior to this analysis, and it was fixed to a grey-level intensity value of 250 for Cy5.5 and Cy3 images.

Feature extraction The quantification of the segmented objects involved implementing a labeling algorithm by selecting more than 1 pixel object and using 8-neighboring pixel clustering for counting object numbers [22,23]. Figure 5 shows the sequence for the quantified image processing. Two main features were summarized, i.e., the number of object and the total object area on an image.

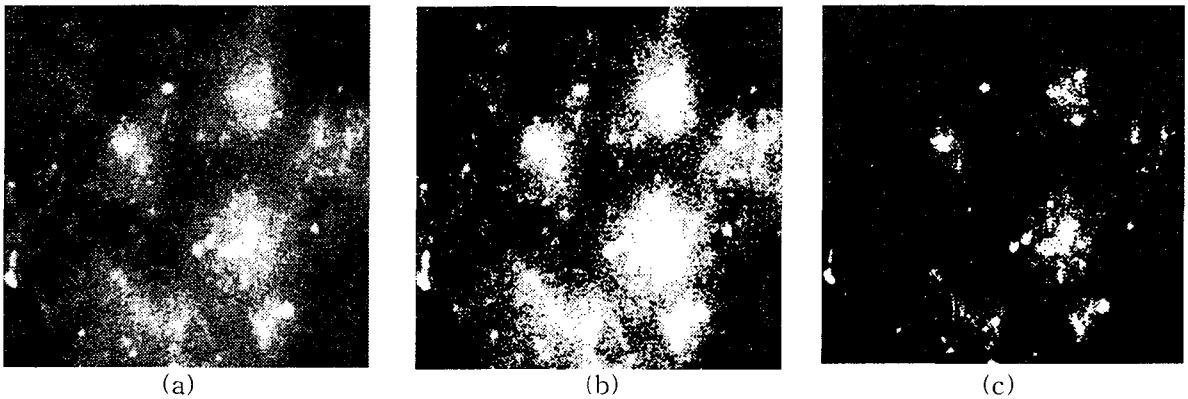

(a) (b) (c)

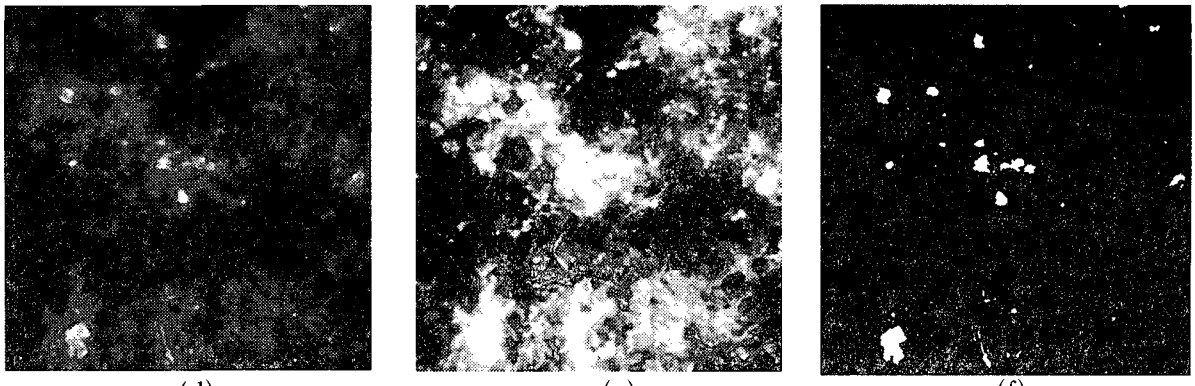

(d) (e) (f)

Figure 5. Image normalisation between LLC and CR-LLC stained with Cy5.5. (a) LLC/Cy5.5 image. (b) The accessed histogram equalisation of image A. (c) After setting the threshold value to 250 of image B. (d) CR-LLC/Cy5.5 image. (e) The accessed histogram equalisation of image D. (f) After setting the threshold value to 250 of image E.

Results

Statistical analysis

Using a multi-variance analysis using the SAS program package [24] we could validate the higher average area and object number for the LLC vs. the CR LLC tumors on all image categories studied. The results are summarized in Table II and Table III together with corresponding concentration values obtained from the FMT studies. Correspondingly there was 1.14%, 1.66% more fluorescence area measured in the Cy 3 and Cy 5.5 channel respectively. In general, LLC has more object numbers than CR-LLC. Only the object numbers of Cy3 in M1 is more CR-LLC than LLC.

Table II Apoptosis quantification of Cy3 and comparison between LLC and CR-LLC
(M1: P> 0.0001, M2: P>0.6576, M3: P>0.0001)

Carcinoma	LLC			CR-LLC		
Features / Mouse	No. Img.	Mean No. Obj.	Mean Area	No. Img.	Mean No. Obj.	Mean Area
M1	10	181	4,719	10	263	4,325
M2	5	191	5,775	5	34	4,372
M3	14	458	4,729	9	97	4,615

Table III Apoptosis quantification of Cy5.5 and comparison between LLC and CR-LLC
(M1: P> 0.0003, M2: P>0.0001, M3: P>0.0001)

Carcinoma	LLC			CR-LLC		
Features / Mouse	No. Img.	Mean No. Obj.	Mean Area	No. Img.	Mean No. Obj.	Mean Area
M1	5	191	5,775	5	34	4,372

M2	6	308	7,493	6	70	4,529
M3	11	341	8,701	10	70	4,295

This demonstrates that apoptosis in an LLC tumor is more spread out throughout a tissue section and each object is generally smaller in size than in CR-LLC tumor sections. In the Tables II and III, No. Img. means the number of images, Mean No. Obj. means mean of the number of objects and Mean Area means mean area of the quantification on an image. The LLC normally has high variance even though the CR-LLC has low variance.

A quantitative comparison between LLC and CR-LLC was simply visualized in graphs in Figure 6. The best discrimination case is Figure 6(a). Also Cy 5.5 is more spread apoptosis on an image and more separable between categorization. The used Cy 5.5 and Cy 3 are sensitive for apoptotic analysis. However their histological images, which are low intensities are not more contrast images than FMT.

Discussion

Macroscopic fluorescence imaging of tissues has attracted significant interest lately since it can record gene expression and molecular function *in vivo* in a non-invasive matter.

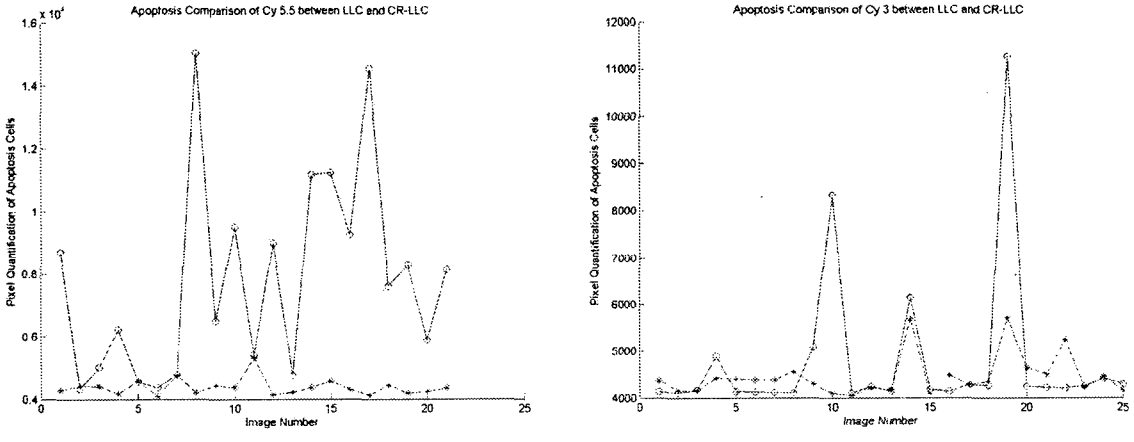

(a) (b)

Figure 6. The apoptosis comparison between LLC(-o) and CR-LLC(--*) in Cy5.5(a) and Cy3 (b).

Small animal imaging has been made possible by the development of planar imaging systems whereas imaging deeper in tissues has been achieved using 3D FMT. As these techniques are evolving, it is important to validate the macroscopic appearance of resolved fluorescence lesions with the underlying microscopy serving as the good standard. In particular, the micro-distribution of the fluorochromes injected *in vivo* can be directly evaluated with NIRfluorescence microscopy. In parallel, immuno-histochemistry studies may independently confirm the targeting capacity by evaluating the micro-distribution of the molecular targets.

In this study we independently evaluated the microscopic appearance of the AnnexinV-Cy5.5 fluorochrome by direct microscopy at the Cy5.5 channel and a corresponding TUNEL assay to evaluate the apoptotic burden of the treated tumors. Vascularization [25] was independently characterized too by *in vivo* injection of Fluor-Lectin prior to animal euthanasia. Computerized

image analysis was central to this work and an important tool to correlate the microscopic appearance to macroscopic FMT findings. Furthermore computer image analysis would also solve the reproducible problem generally. Galliano et al. [26] compared on the slide set with digital set in cervicalvaginal cytology and evaluated interobserver reproducibility. However, a standardized image analysisof the different environment captures is not easy and needs a quantity image data set. The tested algorithm for the percentile method was not robust and oversensitive for intensity variation on an image. And the test auto-contrast algorithm we found an unexpected result. Namely the using histogram equalization and threshold has dared a suitable robust and stability algorithm.

Annexin V labeled with a fluorescent tag is routinely used for histological and cell-sorting studies to identify apoptotic cells [27]. Collingridge et. al. [19] has also synthesized the tumor uptake of Annexin V *in vivo* mouse model apoptosis by PET. In conclusion, the apoptotic images of 3D FMT were validated by histological image analyses. This is a significant result for the continuous progress of fluorescence imaging research.

Acknowledgements

The authors thank Dr. Timothy Browder (Children's Hospital, Harvard Medical School, Boston, MA) for the gift of cyclophosphamide resistant Lewis lung carcinoma variant. Furthermore the authors are grateful to DrsShih Helen, Zacharakis Ioannis, Gordon Turner, Antoine Soubret and zhu banghe for reviewing the manuscript and providing many helpful comments and BS Andreas Yullianno for outstanding technical assistance. This work was supported by the Korea Research Foundation Grant (KRF-2003-013-D00108).

References

1. Weissleder R: Scaling down imaging: molecular mapping of cancer in mice. Nat Rev|Cancer 2002;2:1-8
2. Nakayama A, Bianco AC, Zhang CY, Lowell BB, Frangioni JV: Quantitative of brown adipopse tissue perfusion in transgenic mice using near-infrared fluorescence imaging. Mol Imaging 2003;2:37-49
3. PetrovskyA, Schellenberger E, Josephson L, Weissleder R, Bogdanov A: Near-infrared fluorescent imaging of tumor apoptosis. Cancer Res 2003;63:1936-1942
4. Herschman HR: Molecular imaging: looking at problems, seeing solutions. Science 2003;302:605-608
5. Contag CH, Bachmann MH: Advances in in vivo bioluminescence imaging of gene expression. Annu Rev Biomed Eng 2002;4:235-60
6. Doyle TC, Burns SM, Contag CH: In vivo bioluminescence imaging for intergrated studies of infection. Technoreview 2004;6:303-317
7. K Singbartl, J Thatte, ML Smith, K Wethmar, K Day, K Ley: A CD2-green fluorescence protein-transgenic mouse reveals very late antigin-4-dependent CD 8+ lymphocyte rolling in inflamed venules. J Immunol 2001;166:7520-7526
8. M Yang, L Li, P Jiang, AR Moossa, S Penman, RM Hoffman: Dual-color fluorescence imaging distinguishes tumor cells from induced host agiogenic vessels and stromal cells. PNAS 2003;100:14259-14262
9. Weissleder R, Tung CH, Mohmood U, Bogdanov A Jr.: In vivo imaging of tumors with protease-activated near-infrared fluorescent probes. Nature Biotechnol 1999;17:375-378
10. Bogdanov A, Weissleder R: The development of in vivo imaging systems to study gene

expression. Trends Biotechnol 1998;16:5.-10
11. Bugaj JE, Achilefu S, Dorshow RB, Rajagopalan R: Novel fluorescent contrast agents for optical imaging of *in vivo* tumors based on a receptor-targeted dye-peptide conjugate platform. J Biomed Opt 2001;6:122-133
12. Ntziachristos V, Tung CH, Bremer C, Weissleder R: Fluorescence molecular tomography resolves protease activity in vivo. Nature Med 2002;8:757-761
13. Kerr JF, Wyllie AH, Currie AR: Apoptosis: a basic biological phenomenon with wide-ranging implications in tissue kinetics. Br J Cancer 1972;26: 239-257
14. Vermes I, Haanen C, Steffens-Nakken H, Reutelingsperger C:A novel assay for apoptosis. Flow cytometric detection of phosphatidylserine expression on early apoptotic cells using fluorescein labelled Annexin V. J Immunol Methods1995;184:39-51
15. Blankenberg FG, Strauss HW: Noninvasive imaging using radioactive annexin V is an emerging strategy for the assessment of cell death in vivo. Apoptosis 2001;6:117-123
16. Graves EE, Ripoll J, Weissleder R, Ntziachristos V: A submillimeter resolution fluorescence molecular imaging system for small animal imaging. Med Phys 2003;30:901-911
17. Ntziachristos V, Yodh AG, Schnall M, Chance B: Concurrent MRI and diffuse optical tomography of breast after indo-cyanine green enhancement. Proc Natl Acad Sci USA 2000;97:2767-2772
18. Van de Wiele C, Lahorte C, Vermeersch H, Loose D, Mervillie K, Steinmetz ND, Vanderheyden JU, Cuvelier CA, Slegers G, Dierck RA: Quantitative tumor apoptosis imaging using technetium-99m-HYNIC annexin V single photon emission computed tomography. J Clin Oncol 2003;21:3483-3487
19. Collingridge DR, Glaser M, Osman S, Barthel H, Hutchinson OC, Luthra SK, Brady F, Bouchier-Hayes L, Martin SJ, Workman P, Price P, Aboagye EO: In vitro selectivity, in vivo biodistribution and tumor uptake of annexin V radiolabelled with a positron emitting radioisotope. Br J Cancer 2003;89:1327-1333
20. Gavrieli Y, Sherman Y, Ben-Sasson SA: Identification of programmed cell death in situ via specific labeling of nuclear DNA fragmentation. J Cell Biol 1992;119:493-501
21. Choi HK, Vasko J, Bengtsson E, Jarkrans T, Malmstrom PU, Wester K, Busch C: Grading of transitional cell bladder carcinoma by texture analysis of histological sections. Anal Cell Pathol 6;6:327-343
22. Jason R. Swedlow, Ilya Goldberg, Erik Brauner, PeterK. Sorger: Informatics and quantitative analysis in biological imaging. Science 2003;300:100-102
23. Choi HK, Jarkrans T, Vasko J, Bengtsson E, Malmstroem PU, Wester K, Busch C: Image analysis based grading of bladder carcinoma. Comparision of object, texture and graph based methods and their reproducibility. Anal Cell Pathol 1997;15:1-18
24. Statistical Analysis System(SAS), 8.01, SAS Institute Inc. Cary, NC, USA, 2001.
25. Monsky WL, Fukumura D, Gohongi T, Ancukiewcz M, Weich HA, TorchilinVP, Yuan F, Jain RK: Augmentation of transvascular transport of macromolecules and nano-particles in tumors using vascular endothelial growth factor. Cancer Res 1999;59:4129-4135
26. Tinacci G, Cariaggi MP, Carozzi F, Foggi A, Miccinesi G, Mirri F, Pasquini P, Zappa M, Confortini M: Digital images for interobserver variability comparison in cervicovaginal cytology. Analyt Quant Cytol Histol 2003;25:1-7
27. Vermes I, Haanen C, Steftens-Nakken H, Reutelingsperger: A novel assay for apoptosis: Flow cytometric detection of phosphatidylserine expression on early apoptosis cells using fluorescein-labelled annexin V. J Immunol Methods 1995;184:39-51